JOURNAL OF APPLIED ELECTROCHEMISTRY **27** (1997) 355–363

Kinetics of oxygen reduction at RuO_2-coated titanium electrode in alkaline solution

C. -C. CHANG, T. -C. WEN*

Department of Chemical Engineering, National Cheng Kung University, Tainan,Taiwan 70101

Received 5 January 1996; revised 10 May 1996

Oxygen reduction at RuO_2-coated titanium electrodes prepared by thermal decomposition was investigated by employing cyclic voltammetry and rotating-disc electrode techniques. Cyclic voltammetric results indicated that oxygen reduction was catalysed by at least some hydrous oxyruthenium species, (i.e., Ru(III)) at low polarization range ($E > -0.45$ V) and by at least some low oxide states of ruthenium species at high polarization ($E < -0.45$ V). On the basis of measurements using a rotating disc electrode together with polarization curves, Tafel slopes and stoichiometric number determinations, two mechanisms for oxygen reduction on an RuO_2-coated titanium electrode are proposed.

1. Introduction

Oxygen reduction is an industrially important electrochemical reaction, which is important in fuel cells [1, 2], electrochemical caustic concentrators [3], air depolarized cathodes [4], metal-air batteries [5] and oxidant production [6, 7]. The resultant products from oxygen reduction include either OH^- or HO_2^-, which are reported to be four electron and two electron transfer reaction products, respectively [7]. Thus, the product distribution is determined by the electron transfer pathway, in which the electrocatalyst has the key role.

Recently, several papers [8–12] reported that ruthenium is a good electrode material for oxygen reduction, but that the ruthenium oxide electrode is inactive for oxygen reduction [8–11]. Therefore, almost no attention has been paid to the use of RuO_2 as an oxygen reduction catalyst. However, Adzic *et al.* [9, 11] reported that the oxygen reduction characteristics of partially oxidized Ru, prepared by anodic polarization, could be modified by foreign metal adsorbates. Unfortunately, foreign metals only adsorb on pure Ru metal surfaces, and the surface stability of Ru may not be as good as Ru related alloys. Ru alloys are expensive and not easily obtained. RuO_2/Ti, modified with other metals (e.g., Pb [12], Pt [13], Sn [14], Ir [15]) is easily prepared by thermal decomposition. However, RuO_2/Ti electrochemical behaviour for oxygen reduction has not been studied in detail.

The reasons for the lack of investigations of RuO_2 as a cathode material are obvious. First, the poor conductivity of oxides (compared with pure metal) makes them less attractive as electrode materials. Second, oxides are thermodynamically unstable and will normally be reduced to the metal by hydrogen, which lowers their long-term stability. There is, however, one aspect which makes oxides interesting for application as a cathode material. Oxides, as opposed to pure metals, may be less sensitive to poisoning by foreign metal deposits as a consequence of the surface chemistry. For metals like platinum or nickel, poisoning by metal deposits is well known. The poisoning of cathodes for hydrogen evolution in alkaline media has been investigated by Nidola and Schira [16] who reported that oxidative treatment of the cathode material led to a relative improvement in performance [17]. Kötz and Stucki reported that a RuO_2 cathode in a Membrel electrolysis cell showed more than 4000 h stability and was insensitive to poisoning by metal deposition during hydrogen evolution in acid media.

RuO_2/Ti, used for oxygen reduction, was found to have good current efficiency for H_2O_2 formation [18], but the shape of the response current was different than that of graphite. Therefore, this work was designed to elucidate the mechanism of oxygen reduction on RuO_2/Ti electrodes in alkaline solution.

2. Experimental details

2.1. *Preparation of RuO_2 electrode*

Preparation of RuO_2-coated titanium electrodes was similar to that described in previous work [19]. The substrate was polished with silicon carbide paper (600 grit down to 1200 grit), washed with ethanol in an ultrasonic cleaner, polished with 0.3 μm alumina–water suspension, washed with ethanol in an ultrasonic cleaner, etched for 20 min in a 3 M HCl solution at 80 to 90 °C, and finally washed and stored in ultrapure water. Following these procedures, the substrates were dipped in coating solution which consisted of $RuCl_3.xH_2O$ (Johnson Matthey, 42.25% metal content) at a total concentration of 0.25 mol dm^{-3} with 10% by volume concentrated HCl (Merck, G.R.) in isopropanol (Merck, G.R.). After dipping and drying, the titanium substrates were heated under

* To whom correspondence should be addressed.

0021-891X

air flow at an annealing temperature of 450 °C for 10 min. The entire procedure was repeated five times, after which the substrate was heated at the annealing temperature for one hour. The total oxide loading of these electrodes was normally around 0.7 ~ 0.9 mg cm^{-2}. The RuO_2 coated disc was assembled into a Teflon cylindrical tube with a 6 mm inner diameter, as per Chang and Wen [20]. To avoid electrolyte leakage, the entire assembly between disc and Teflon tube was sealed with epoxy cement.

2.2. *Electrochemical studies*

Rotating disc electrode experiments were carried out with a BAS-100B potentiostat/galvanostat system with a BAS rotating disc electrode (Bioanalytical System, USA). An Ag/AgCl electrode (Bioanalytical System, 3 M KCl, 0.207 V vs NHE at 25 °C) was used as the reference, and a platinum wire was employed as the counter electrode. A Luggin capillary with its tip ~ 3 mm below the centre of the rotating disc electrode was used to minimize the *iR* drop. All solutions were prepared with ultrapure water produced by a reagent water system (Milli-Q SP, Japan) at 18 MΩ cm^{-1}. All chemicals were Merck G.R. reagents and potentials are quoted against the Ag/AgCl reference electrode. The various pH solutions were prepared from special low carbonate KOH pellets and K_2SO_4 with an approximately constant ionic strength of unity. The dissolved oxygen concentration was controlled by adjusting the ratio of oxygen to nitrogen of a bubbling gas flow at a total flow rate of 625 ml min^{-1} and measured by an oxygen-meter (WTW-OXI 96, Germany). The *i*/*E* curves of the RuO_2 coated rotating disc in various pH solutions were obtained by linear sweep voltammetry, from approximately 0.2 V more than open-circuit potential to −1.2 V vs Ag/AgCl at 1 mV s^{-1}. All measurements were taken at 25 °C (accuracy of 0.05 °C) with a water thermostat (HAAKE D8 and G).

2.3. *Potentiostatic electrolysis*

Potentiostatic electrolysis was carried out in a divided cell with a Nafion® 435, a platinum wire, and one of the thermally prepared electrodes as separator, counter electrode, and working electrode, respectively. A 20 cm^2 working surface area was delimited by double coating the surplus surface area with epoxy cement. In the steady state oxygen reduction experiments, the various potentials were controlled by a HA-301 potentiostat/galvanostat system (Hokuto Denko Company, Japan). After electrolysis, the hydrogen peroxide concentration in the electrolytic product was determined by titrating an acidified 1 ml aliquot with 0.02 M potassium permanganate solution.

3. Results and discussion

3.1. *Cyclic voltammetry*

Typical cyclic voltammograms of an RuO_2-coated electrode in 1 M KOH solution with bubbling N_2 or O_2 at a scan rate of 100 mV s^{-1} are shown in curves 1 and 2 of Fig. 1, respectively. Curve 1 shows four paired regions, which are attributed to the specific redox transitions of surface hydrous oxyruthenium groups characteristic of a given potential range, that is, Ru(VI)/Ru(VII), Ru(IV)/Ru(VI), Ru(III)/Ru(IV), and Ru(0)/Ru(III), as reported previously [21–23]. Comparing curve 1 to curve 2, it is easily seen that the Ru(VI)/Ru(VII) and Ru(IV)/Ru(VI) regions exhibit essentially identical characteristics (excepting the extreme negative end of the potential scale, which is a

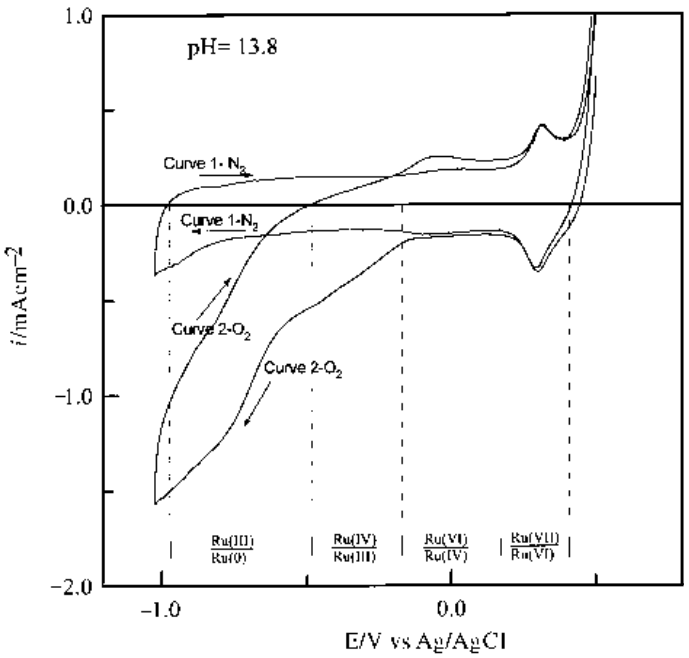

Fig. 1. Cyclic voltammograms of an RuO_2/Ti electrode in 1 M KOH solution with a scan rate of 100 mV s^{-1} at 25 °C, saturated with bubbling: (1) N_2 and (2) O_2.

special region of hydrogen adsorption), but that the activities in the Ru(III)/Ru(IV) and Ru(0)/Ru(III) regions are dramatically different. The Ru(III)/Ru(IV) and Ru(0)/Ru(III) regions of curve 1, show essentially constant current, but in the same regions curve 2 a slope occurs. The slope in curve 2 Ru(0)/Ru(III) (slope = 2.05) region is approximately double that in curve 2 Ru(III)/Ru(IV) (slope = 1.03) region. The difference in slopes may be due to the fact that two electron transfer occurs in the Ru(III)/Ru(IV) region while four electron transfer occurs in the Ru(0)/Ru(III) region. It also implies that two mechanisms and/or two kinds electrocatalysts exist at RuO_2-coated electrodes. Adzic *et al*. [9, 11] reported that Ru oxide obtained from anodization of Ru is inactive for oxygen reduction. This differing result may be due to the different preparation methods. In this work, CV results (Fig. 1) obviously indicate two reactive regions for oxygen reduction. This information, coupled with this laboratory's interest in RuO_2/Ti electrodes, stimulated the following rotating disc experiments, performed to elucidate the mechanisms of oxygen reduction at low polarization ($-0.10 \sim -0.45$ V) and high polarization ($-0.45 \sim -0.90$ V).

3.2. *Rotating disc data*

Figures 2 and 3 show the rotating disc (RuO_2/Ti) data for oxygen reduction at pH 10.8 and 13.8, respectively. The data were obtained by sweeping the potential in the negative direction at 1 mV s^{-1}. A slow sweep rate was used to avoid possible interference from redox processes, that is, Ru(IV)/Ru(III) and Ru(III)/Ru(0) redox, occurring simultaneously with oxygen reduction. Comparisons between curve (f) and curve (f′) in Figs 2 and 3 show that no competitive current occurs at potentials from 0.00 to −0.95 V; the background currents are insignificant and are therefore neglected. All curves are similar in shape (S-shape) for other pH solutions. A comparison of the magnitude of currents between Figs 2 and 3 indicates that the oxygen reduction rate at low polarization in high pH solution (pH 13.8) is larger than that in low pH solution (pH 10.8). The oxygen reduction rate at high polarization in high pH solution (pH 13.8) is smaller than that at low pH (pH 10.8). With the results of CV data in mind, the former result is attributable to the higher electrocatalytic activity of Ru(III) for oxygen reduction at high pH than at low pH, explained by the fact that OH^- ions are involved during oxygen reduction at Ru(III). The latter result is possibly due to oxygen reduction at the low oxide state of ruthenium producing OH^- ions.

3.3. *Reaction order with respect to O_2*

The reaction order with respect to dissolved oxygen can be determined by varying the concentration of dissolved oxygen [24], which is plotted against the partial pressure of oxygen at constant potential and constant rotation rate (here, 4000 rpm), as in Fig. 4. It should be noted that the kinetic current density, i_k, was obtained by correction for diffusion effects using the relation,

$$i_k = \frac{i i_L}{i_L - i} \tag{1}$$

where i_k is the current density corrected for diffusion effects, i.e., the kinetic current density [24], i is the disc

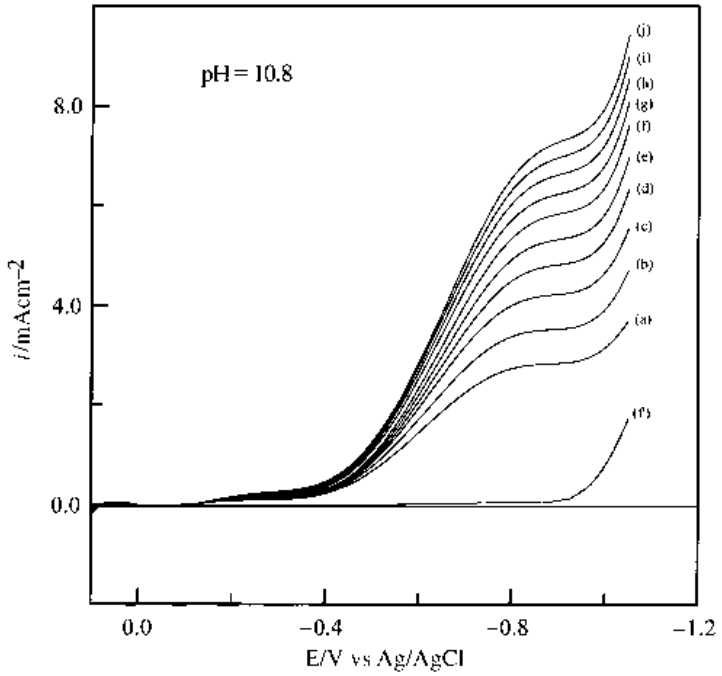

Fig. 2. Polarization curves for oxygen reduction on an RuO_2 electrode in 0.001 M KOH solution recorded in the negative direction at a scan rate of 1 mV s^{-1}. Specified rotation rates: (a) 500, (b) 1000, (c)1500, (d) 2000, (e) 2500, (f) 3000, (g) 3500, (h) 4000, (i) 4500 and (j) 5000 rpm. The line (f′) is in purged N_2 electrolyte at 3000 rpm.

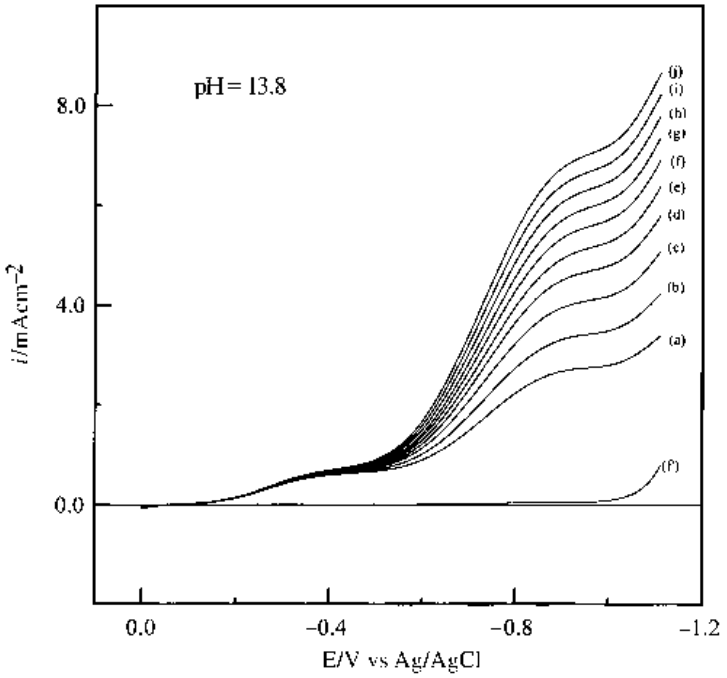

Fig. 3. Polarization curves for oxygen reduction on an RuO_2/Ti electrode in 1 M KOH recorded in the negative direction at a scan rate of 1 mV s^{-1} at rotation rates as specified in Fig. 2.

current density, and i_L is limiting current density. Equation 1 can be employed only when the reaction is under mixed activation-diffusion control. The slope of the straight line plots shown in the diagram is close to 1 in the potential range −0.10 to −0.85 V, indicating a first order reaction with respect to O_2.

3.4. *Apparent number of electrons exchanged per O_2 molecule*

For a first order reaction with respect to dissolved oxygen, the disc current i is related to rotation rate ω by the following equation [25]

$$\frac{1}{i} = \frac{1}{i_k} + \frac{1}{0.62\, nFD_0^{2/3} C_b \nu^{-1/6} \omega^{1/2}} \qquad (2)$$

where n is the number of electrons transferred per molecule of O_2, F is the Faraday constant (96 500 C mol^{-1}), C_b is the bulk oxygen concentration (1.103×10^{-3} M [26]), D_0 is the diffusion coefficient of molecular oxygen (1.76×10^{-5} cm^2 s^{-1} [26]), v is the kinematic viscosity (~ 0.01 cm^2 s^{-1} for the solvent) and ω is the electrode rotation rate. Typical i^{-1} against $\omega^{-1/2}$ plots are shown in Fig. 5(a) and (b) for pH 10.8 and 13.8, respectively. At high polarization, slopes in Fig. 5(a) or (b) with $n = 4$ can be fitted over a wide rotation frequency interval. At low polarization, slopes with $n = 2$ or nearly $n = 4$ can be observed at high and low rotating rates respectively. This causes the bending of the i^{-1} against $\omega^{-1/2}$ plots, at low polarization, reflecting the change in electron transfer number that accompanies change in rotational frequency, thereby providing evidence of a complex reaction mechanism for the overall cathodic reaction. These results are similar to those obtained previously [20, 27]. At high polarization, there exist non-zero intercepts on the ordinate, as reported by Landsberg *et al.* [28] and Taylor *et al.* [29].

On the basis of the above results, oxygen reduction appears to proceed by an overall four electron transfer process without peroxide generation at high polarization. On the other hand, oxygen reduction proceeds via a two electron transfer process (i.e., forming HO_2^-) at low polarization with high rotation rates. It is conceivable that oxygen adsorption on Ru(III) is end on [10, 30], and then is reduced to a peroxide species which can either be desorbed as HO_2^- or further reduced to OH^-. At high polarization,

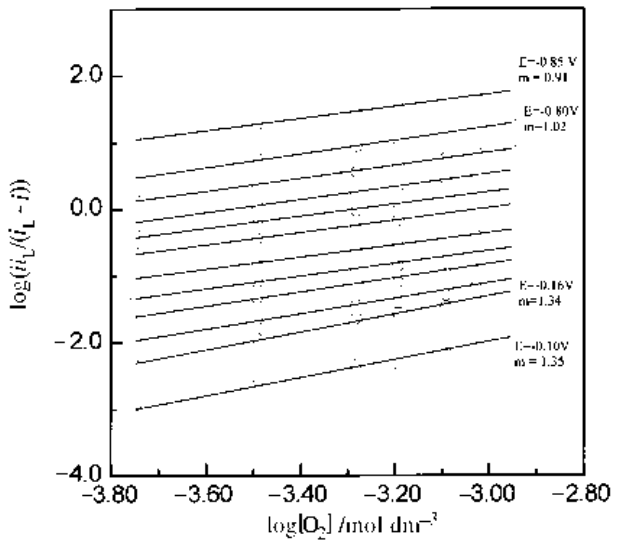

Fig. 4. Plot of log $[O_2]$ against log $[i i_L/(i_L - i)]$ for oxygen reduction on an RuO_2/Ti electrode in 1 M KOH solution at various potentials.

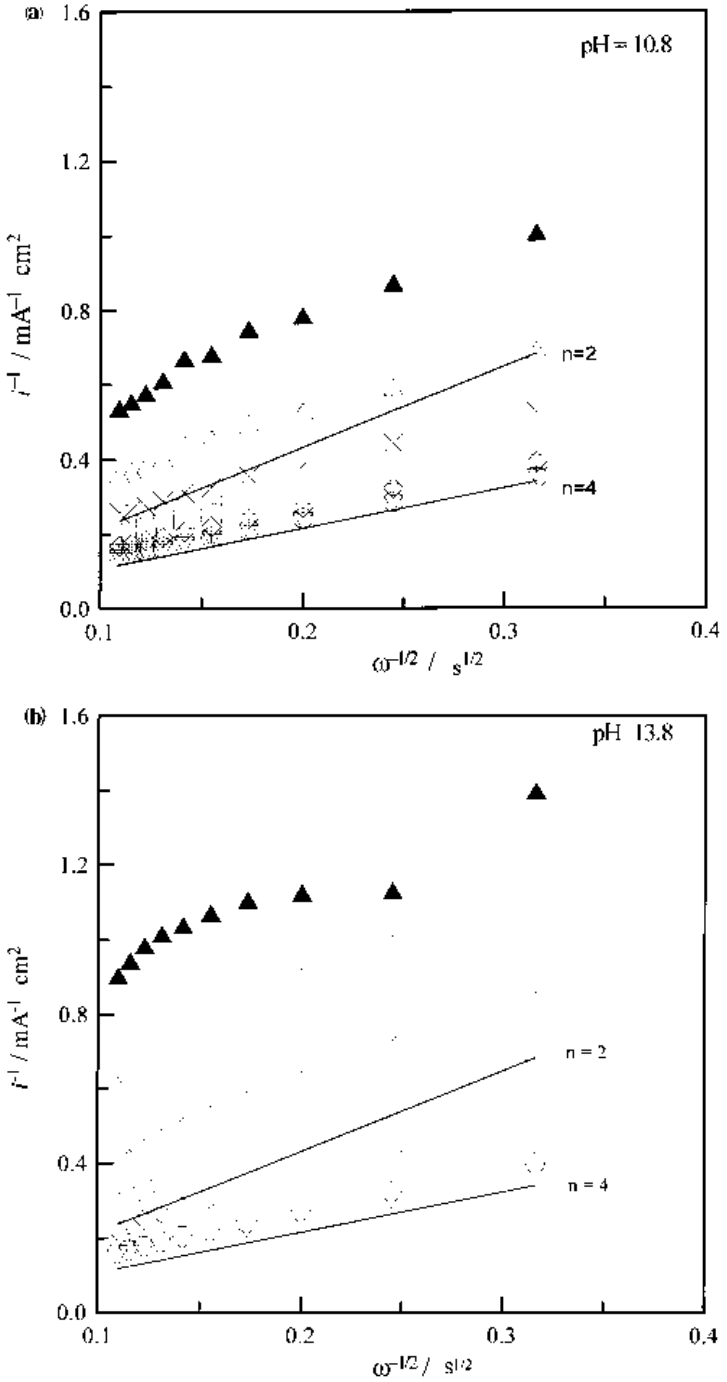

Fig. 5. Plots of i^{-1} against $\omega^{-1/2}$ for an RuO_2/Ti electrode in (a) 0.1 M KOH and (b) 1 M KOH solutions with O_2 (1 atm) at different potentials. Solid line: calculated from Equation 2 for $n = 2$ and $n = 4$. Key:(▲) − 0.55, (△) − 0.60, (×) − 0.65, (□) − 0.70, (◇) − 0.75, (+) − 0.80, (○) − 0.85, and (▽) − 0.90 V.

oxygen adsorbed on the ruthenium low oxide state can be directly reduced to OH^- [8–10] and/or proceed via a pair of two electron transfers to OH^-.

3.5. *Tafel slopes*

Figure 6 shows two straight-line regions in the plot of E against log $[i/(i_L - i)]$ for solutions of various pH. In order to avoid the influence of hydrogen evolution on oxygen reduction, a potential of −0.90 V (at 4000 rpm) was chosen for the limiting current densities (i_L) 6.25, 6.13, 5.72 and 5.35 mA cm^{-2} at their respective pH values of 10.8, 11.9, 12.9 and 13.8. At low polarization, the slopes of the lines in the pH range 13.8–10.8 are essentially the same and range from −260 to −280 mV dec^{-1}. Meanwhile, at high polarization, the slopes were about −150 mV dec^{-1}. Slopes with absolute values larger than 120 mV dec^{-1} are attributable to RuO_2 different nature and mechanisms in different potential regions. Similar results were reported by Anastasijevic *et al.* [8,10]. It seems that the value of the slope is very sensitive to the oxidation state of the Ru surface. Therefore, at high polarization, the presence of a low Ru oxide state on a RuO_2/Ti electrode causes a small slope (−150 mV dec^{-1}), while at low polarization, a high oxidation

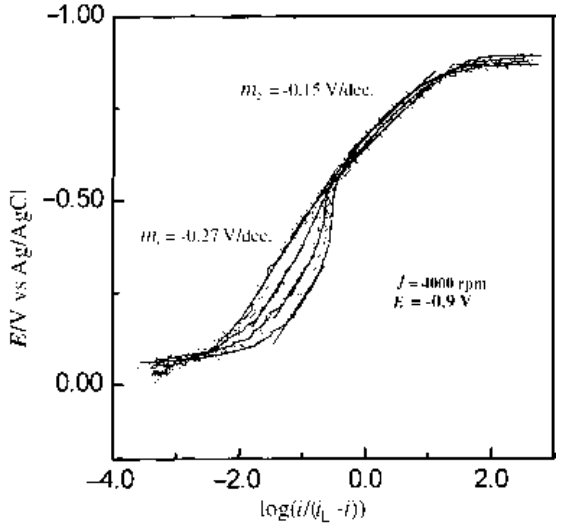

Fig. 6. Tafel plots of log $[i/(i_L-i)]$ against E for O_2 reduction on an RuO_2/Ti electrode in various pH solutions at a rotation rate of 4000 rpm. pH, i_L: (◇) 10.8 at 6.25 mA cm^{-2}; (□) 11.9 at 6.13 mA cm^{-2}; (△) 12.9 at 5.72 mA cm^{-2}; (○)13.8 at 5.35 mA cm^{-2}.

state of hydrous oxyruthenium species, i.e. Ru(III), causes a large slope (−200 ~ −300 mV dec^{-1}). When a low negative potential is applied to the RuO_2/Ti electrode (Ru(III) state), there are many OH^- ions and H_2O molecules around the electrical double layer to hinder oxygen adsorption/electron transfer and possibly change the oxygen reduction pathway, causing these high Tafel slopes (−200 ~ −300 mV dec^{-1}). On the other hand, at high polarization, high negative potential drive OH^- and H_2O out of the double layer, thereby facilitating oxygen adsorption/electron transfer. This situation coupled with the low oxide state of Ru would then give a −150 mV dec^{-1} Tafel slope with a four electron transfer process.

3.6. *Reaction order with respect to OH^-*

Figure 6 reveals that at high polarization, the curves of E against log $[i/(i_L-i)]$ are close to each other. At high polarization, the reaction order with respect to OH^- concentration over the pH range 10.8–13.8 is thus of approximately zero order. On the other hand, at low polarization the curves of E against log $[i/(i_L-i)]$ for various pH values are strongly dependent on pH.

Since the reaction is first order in O_2 concentration and the activity of water for solutions of different pH is essentially constant, the rate of the reaction can be expressed as a kinetic current density:

$$i_k = k\,[O_2][OH^-]^r \qquad (3)$$

where the back reaction is negligible. For a first-order reaction in O_2, i_k can be also derived from Equation 1. Using Equations 1 and 3, the reaction order for OH^-, r, can be obtained through the first derivative as the following equation:

$$r = \left(\frac{\partial \log i_k}{\partial \log[OH^-]}\right)_E = \left(\frac{\partial \log(i/(i_L - i))}{\partial \log[OH^-]}\right)_E \qquad (4)$$

The plots of log $[i/(i_L-i)]$ against log $[OH^-]$ for the low polarization-Tafel linear region in Fig. 6 yield straight lines over the pH range 13.8 to 10.8 (Fig. 7). From the slope of the curves, a reaction order of approximately 0.25 is found with respect to OH^- concentration for oxygen reduction. This 0.25 OH^- concentration reaction order may be attributed to two causes: (i) the supernernstian potential–pH behaviour of the Ru(IV)/Ru(III) transition [21] and (ii) the adsorption of oxygen via Temkin's proposed behaviour [31, 32]. This concept is similar to the behaviour of oxygen reduction on IrO_2-coated titanium electrode [20].

3.7. *Mechanistic considerations*

On the basis of the above results and discussion, the mechanism of oxygen reduction at low polarization can be assumed to differ from that at high polarization. We conclude that oxygen reduction is catalysed by hydrous oxyruthenium species in the low polarization range ($E > -0.45$ V) and by low oxide state ruthenium in the high polarization range ($E < -0.45$ V). The reaction at low polarization is strongly dependent on pH and has an order of 0.25 in OH^- concentration over the pH range 13.8–10.8. In contrast, the process at high polarization is practically pH independent over the entire studied range (13.8–10.8). Both processes are first order in oxygen. It is clear that there are two potential regions for oxygen reduction. One, based on the model of a hydrous oxyruthenium catalyst [30], is observed at low polarization. The other, based on O_2 adsorption on low oxide oxyruthenium species (e.g., Ru metal catalyst), is observed at high polarization [8–11].

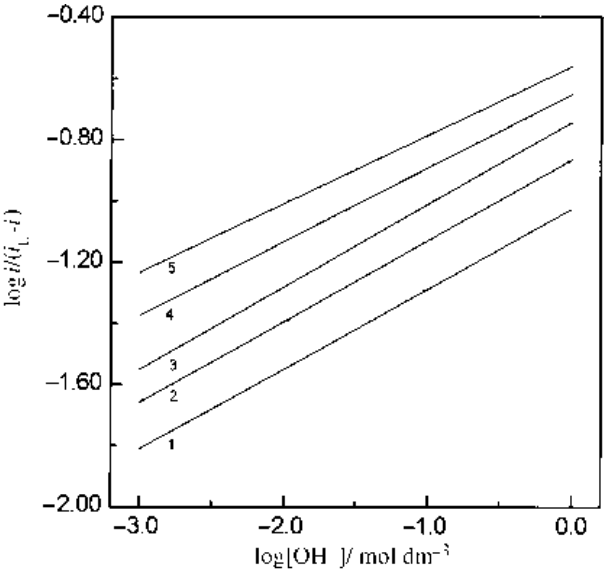

Fig. 7. log $[i/(i_L-i)]$ as function of experimentally modified OH^- concentration at constant applied voltages. The values of $i/(i_L-i)$ taken from the Tafel linear region of low polarization in Fig. 6, extrapolated, if necessary, at a constant potential. Applied voltage: (1) −0.22, (2) −0.26, (3) −0.30, (4) −0.34 and (5) −0.38 V.

3.7.1. Hydrous oxyruthenium catalyst model. According to the hydrous oxyruthenium catalyst model, the surface of oxyruthenium species in electrolytes is covered by OH groups and H_2O molecules. The adsorption of O_2 molecules on Ru(III) active centres is hindered by the steric hindrance of the OH/H_2O surface layer. However, assuming the active centre S on hydrous oxyruthenium species (i.e., Ru(III)) are $Ru(OH)_3$ which can adsorb O_2 molecules as $Ru(OH)_3 \cdot O_2$, a possible reaction scheme is

$$Ru(OH)_3 + O_2 \rightleftharpoons [Ru(OH)_3].O_{2(ads)} \quad (5)$$

$$[Ru(OH)_3].O_{2(ads)} + x\,OH^- + e^- \longrightarrow [Ru(OH)^{-x}_{(3+x)}].O^-_{2(ads)} \quad (6)$$

$$[Ru(OH)^{-x}_{(3+x)}].O^-_{2(ads)} + H_2O + e^- \rightleftharpoons [Ru(OH)_3].O_2H^-_{(ads)} + (1+x)\,OH^- \quad (7)$$

$$[Ru(OH)_3].O_2H^-_{(ads)} \rightleftharpoons Ru(OH)_3 + HO_2^- \quad (8)$$

$$[Ru(OH)_3].O_2H^-_{(ads)} + H_2O + 2e^- \rightleftharpoons Ru(OH)_3 + 3OH^- \quad (9)$$

The adsorption of oxygen on hydrous oxyruthenium species is a fast step (Reaction 5). During Reaction 6 the transfer of one mole of electrons from adsorbed oxygen on hydrous oxyruthenium takes x moles of OH^- ions from the bulk solution. This has a reaction order value of 0.25 for oxygen adsorption on hydrous oxyruthenium, as observed in this work. In addition, Reaction 6 is the rate-determining step since the rate-determining process is O_2 (physisorbed) + e^- $\rightarrow$ O_2^- (chemisorbed), that is, simultaneous electron transfer and chemisorption [25, 33]. Reaction 7 would then follow and be followed by further fast steps, finally yielding HO_2^- or OH^- (respectively, Reactions 8 or 9) as the product of the O_2 reduction, with a total of $2e^-$ or $4e^-$ per O_2 consumed. Meanwhile, $Ru(OH)^{-x}_{(3+x)}$ is returned to $Ru(OH)_3$. According to our proposed reaction scheme, the rate equation for oxygen reduction on the RuO_2-coated titanium electrode can be expressed as

$$i = k_6 K_5 F [Ru(OH)_3][O_2][OH^-]^{0.25} \exp\left(-\frac{\alpha F}{RT}\eta_6\right) \quad (10)$$

or

$$i = i_L [O_2][OH^-]^{0.25} \exp\left(-\frac{\alpha F}{RT}\eta_6\right) \quad (11)$$

where $i_L = k_6 K_5 F\,[Ru(OH)_3]$, $Ru(OH)_3$ is the surface concentration of hydrous oxyruthenium species, α is the symmetry factor (0.5), $\eta_6 = E - E_{06}$ is the overpotential, E_{06} is the standard electrode potential, k_6 is the rate constant at the standard electrode potential for Reaction 6 that is, $E = E_{06}$, K_5 is the equilibrium rate constant for Reaction 5, and F, R and T have their usual meanings. For $\alpha = 0.5$, the Tafel slope is -120 mV dec^{-1}. This is different from our experimental data, that is, -270 mV dec^{-1}. This behaviour can be explained by the inhibiting influence of the thick layer of Ru oxide on oxygen reduction, which was discussed above. Equation 11 predicts the essential features of the experimental data below the high polarization, Tafel-linear region in the pH range from 10.8 to 13.8. The reaction orders are one for $[O_2]$, 0.25 for $[OH^-]$, thus predicting a limiting current density i_L that is directly proportional to the surface concentration of hydrous oxyruthenium species.

3.7.2. Low oxide state of oxyruthenium catalyst model. The reaction model is based on the adsorption of O_2 molecules on centres of low Ru oxide state. According to this model, hydrous oxyruthenium species may be reduced to the low oxide state by high cathodic polarization, and then O_2 molecules are directly adsorbed on low oxide state ruthenium. A direct $4e^-$ reduction requires metal —O_2 interaction in a 'bridge' configuration, which may lead to O—O bond scission. Such interaction with a partially oxidized Ru surface can be envisaged only through a formation of the 'sandwich' type structures as in metal/oxygen/metal [8–11]. The possible reaction mechanisms for O_2 reduction at high overpotential are proposed as follows:

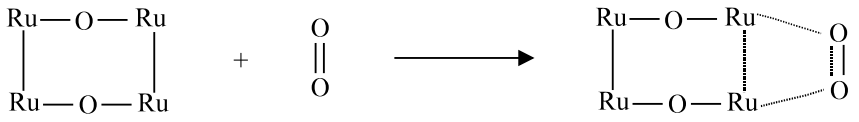

(12)

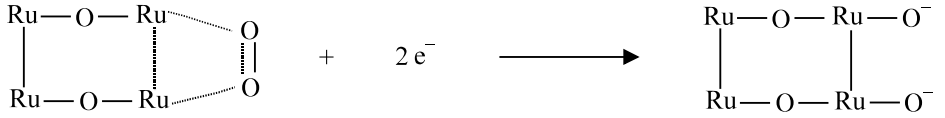

(13)

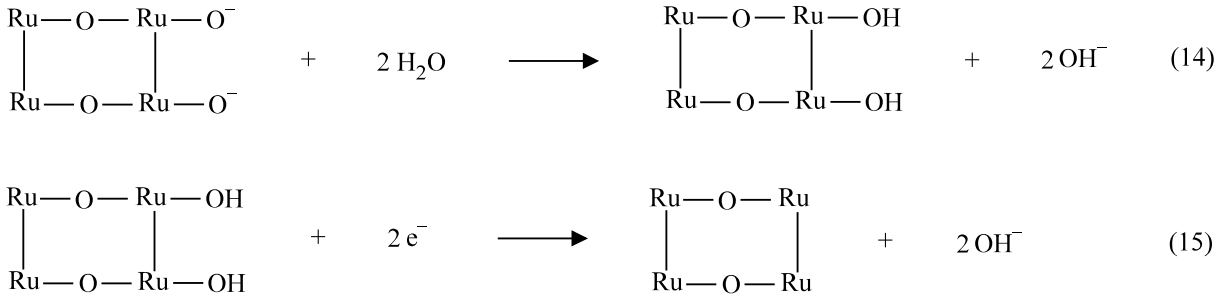

Reaction 12 might be followed by a slow charge transfer step, Reaction 13, which is the rate-determining step. During Reaction 13, the low oxide state of ruthenium can function as an electron transfer mediator which transfers electrons to oxygen and is necessary for rupture of the O—O bond. Reaction 14 would then be followed by further fast steps to decompose the H_2O to OH^- and then transfer two electrons to the adsorbed –OH, finally yielding OH^- in Reactions 15. The theoretical value of about −120 mV dec^{-1} Tafel slope for Reaction 13 (our proposed first electron transfer step) strongly indicates that it is a rate determining step. The higher Tafel slope value (−150 mV dec^{-1}) observed experimentally is close to the theoretical value. The difference may be explained by the 'sandwich' structure, that is, by the presence of subsurface oxygen and the resulting potential drop in the oxide layer [8–11]. Thus, the rate equation for oxygen reduction at high polarization can be expressed as

$$i = i_L[O_2]\exp\left(-\frac{\alpha F}{RT}\eta_{13}\right) \qquad (16)$$

where $i_L = k_{13}K_{12}F$ [Ru—O—Ru], [Ru—O—Ru] is the surface concentration of low oxide state ruthenium species, α is the symmetry factor (0.5), $\eta_{13} = E - E_{013}$ is the overpotential, E_{013} is the standard electrode potential, k_{13} is the rate constant at the standard electrode potential for Reaction 13 (i.e., at $E = E_{013}$), and K_{12} is the equilibrium rate constant for the Reaction 12. For $\alpha = 0.5$, the Tafel slope is −120 mV dec^{-1}. This theoretical value is a little different from our experimental value of −150 mV dec^{-1}, which can be explained by the influence of the thin layer of Ru oxide on oxygen reduction, as discussed above. Equation 16 predicts the essential features of the experimental data in the high polarization-Tafel linear region in the pH range from 10.8 to 13.8. The reaction order is one for $[O_2]$, zero for $[OH^-]$, and predicts a limiting current density i_L that is directly propotional to the surface concentration of low oxide state ruthenium.

3.8. *Hydrogen peroxide current efficiency*

According to the above discussion, the electrocatalyst species active in oxygen reduction on the RuO_2-coated titanium electrode were hydrous oxyruthenium species (i.e., Ru(III), at low polarization) and low oxide state of ruthenium (at high polarization). Oxygen reduction on hydrous oxyruthenium species is considered to proceed primarily through a two electron pathway, while that on low oxide state ruthenium species proceeds primarily through a four electron pathway. Therefore, the major product is dependent on the electrocatalytic properties of the electrode's active surface species.

The dependence of hydrogen peroxide current efficiency on the electrode potential for oxygen reduction in 1 M KOH solution containing saturated oxygen is shown in Fig. 8. The H_2O_2 current efficiency at approximately −0.45 V decreases rapidly from 43% to 8%. This can be attributed to the different electrocatalytic activities of hydrous oxyruthenium species for oxygen reduction at different potentials. The RuO_2-coated electrode in the potential range from −0.10 to −0.90 V (see Fig. 1) has hydrous oxyruthenium species (i.e., Ru(III), in the potential range from −0.10 to −0.45 V) and low oxide state ruthenium species (i.e., Ru—O—Ru, at potentials < −0.45 V). This indicates that, at potentials > −0.4 V, oxygen reduction on hydrous oxyruthenium species (i.e., Ru(III)) primarily proceeds through two electron transfer with a final product of approximately 58% HO_2^- and 42% OH^-, suggesting that the products OH^- and HO_2^- might have

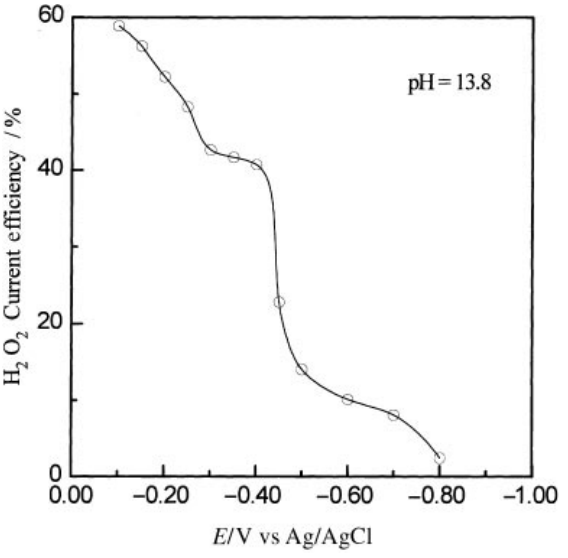

Fig. 8. The current efficiency of H_2O_2 production as a function of electrode potentials for O_2 reduction on an RuO_2/Ti electrode. Hydrogen peroxide current efficiencies were obtained by passing 100 C in 1 M KOH solution containing saturated oxygen.

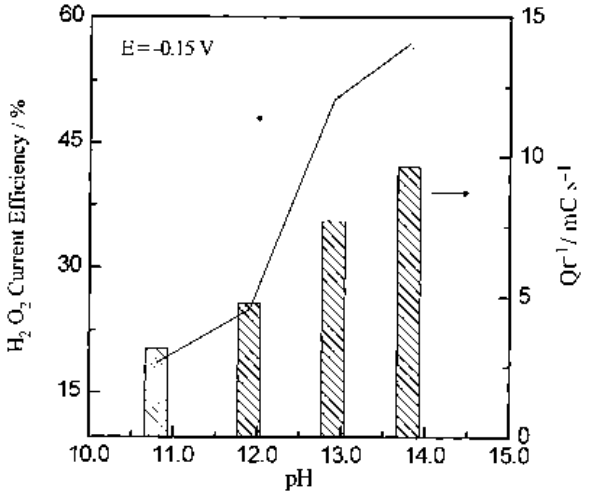

Fig. 9. Current efficiencies for H_2O_2 production (line) and passing charge rates (bars) for oxygen reduction on an RuO_2/Ti electrode obtained by passing 100 C in various KOH concentrations containing saturated oxygen at −0.15 V.

approximately equal opportunities to form in the low polarization region. However, at potentials < −0.40 V, oxygen reduction on low oxide state Ru operates predominantly through a four-electron direct reduction to approximately 90% OH^-.

Current efficiencies for H_2O_2 production and charge rates for the O_2 reduction reaction at various KOH concentrations at a constant potential (−0.15 V) are shown in Fig. 9 by the curve and bars respectively. The current efficiency for H_2O_2 production increases with increasing KOH concentration, supporting the premise that Reaction 9 is inhibited by high OH^- concentration. An examination of the bar graph in Fig. 9 shows that passing charge rates for O_2 reduction increase with increasing OH^- concentration. This result confirms that electrocatalytic activity for oxygen reduction on hydrous oxyruthenium species (i.e., Ru(III)) at high (pH 13.8) is better than that at low pH (pH 10.8).

4. Conclusion

Oxygen reduction on RuO_2-coated titanium electrodes in alkaline solutions from pH 10.8 to 13.8 are catalysed by hydrous oxyruthenium species, that is, Ru(III), at low polarization (−0.1 ~ −0.45 V) and by low oxide state oxyruthenium species at high polarization (−0.45 ~ −0.90 V). In the low polarization region, oxygen reduction with a Tafel slope of −270 mV dec^{-1} depends on the solution pH and has an OH^- reaction order of 0.25 when in the pH range of 10.8 to 13.8. In the high polarization region, oxygen reduction proceeds with a Tafel slope of −150 mV dec^{-1} and the process is practically pH independent. Both cases are first order in dissolved O_2. At low polarization, the major product of oxygen reduction is hydrogen peroxide.

Acknowledgements

Financial support of this work by the National Science Council of the Republic of China under Contract No NSC 85-2214-E006-026, and English consultation by Randy Gillespie are acknowledged.

References

[1] J. C. Huang, R. K. Sen and E. Yeager, *J. Electrochem. Soc.* **126** (1979) 786.
[2] J. M. Zen, R. Manoharan and J. B. Goodenough, *J. Appl. Electrochem.* **22** (1992) 140.
[3] N. R. K. Vilambi and E. J. Taylor, *Separation Sci. Technol.* **25** (1990) 627.
[4] M. Sudoh, T. Kodera, H. Hino and H. Shimamura, *J. Chem. Eng. Japan* **21** (1988) 198.
[5] C. C. Wang, K. S. Goto and S. A. Akbar, *J. Electrochem. Soc.* **138** (1991) 3673.
[6] J. J. Jow, A. C. Lee and T. C. Chou, *J. Appl.Electrochem.* **17** (1987) 753.
[7] C. Oloman and A. P. Watkinson, *ibid.* **9** (1979) 117.
[8] N. A. Anastasijevic, Z. M. Dimitrijevic and R. R. Adzic, *J. Electroanal. Chem.* **199** (1986) 351.
[9] R. R. Adzic, N. A. Anastasijevic and Z. M. Dimitrijevic, *J. Electrochem. Soc.* **131** (1984) 2730.
[10] N. A. Anastasijevic, Z. M. Dimitrijevic and R. R. Adzic, *Electrochimica Acta* **31** (1986) 1125.
[11] *Idem, ibid* **37** (1992) 457.
[12] H. S. Horowitz, J. M. Longo and H. H. Horowitz, *J. Electrochem. Soc.* **130** (1983) 1851.
[13] C. Comninellis and G. P. Vercesi, *J. Appl. Electrochem.* **21** (1991) 136.
[14] J. F. C. Boodts and S. Trasatti, *J. Electrochem. Soc.* **137** (1990) 3784.
[15] C. Angelinetta and S. Trasatti, *Mater. Chem. Phys.* **22** (1989) 231.
[16] A. Nidola and R. Schira, *J. Electrochem. Soc.* **133** (1976) 1653.
[17] F. Y. Masuda, *J. Appl. Electrochem.* **16** (1986) 317.
[18] C. C. Chang and T. C. Wen, *Mater. Chem. Phys*. in press (1996).
[19] S. M. Lin and T. C. Wen, *Electrochim. Acta* **39** (1993) 393.
[20] C. C. Chang and T. C. Wen, *J. Electrochem. Soc.* **143** (1995) 1473.
[21] L. D. Burke and J. F. Healy, *J. Electroanal. Chem.* **124** (1981) 327.
[22] T. C. Wen and C. C. Hu, *J. Electrochem. Soc.* **139** (1992) 2158.
[23] D. Galizzioli, F. Tantardini and S. Trasatti, *J. Appl. Electrochem.* **4** (1974) 57.
[24] S. Lj Gojkovic, S. K. Zecevic, and D. M. Drazic, *Electrochim. Acta* **39** (1994) 975.
[25] V. G. Levich, 'Physiochemical Hydrodynamics', Prentice Hall, Englewood Cliffs, NJ (1962).
[26] K. E. Gubbins and R. D. Walker, Jr, *J. Electrochem. Soc.* **112** (1965) 469.
[27] E. R. Vago and E. J. Calvo, *J. Electroanal. Chem.* **339** (1992) 41.
[28] R. Landsberg and H. Thiele, *Electrochim. Acta* **11** (1966) 1243.
[29] R. J. Taylor and A. A. Humffray, *J. Electroanal.Chem.* **64** (1975) 63.
[30] A. C. C. Tseung, *J. Electrochem. Soc.* **125** (1978) 1660.
[31] D. B. Sepa, M. V. Vojnovic and A. Damjanovic, *Electrochim. Acta* **26** (1981) 781.
[32] A. Damjanovic and V. Brusic, *ibid.* **12** (1967) 615.
[33] V. S. Bagotzky, N. A. Shumilova and E. L. Khrushcheva, *ibid.* **21** (1976) 919.